Innovations in applied physics

Izvestiya Vysshikh Uchebnykh Zavedeniy. Applied Nonlinear Dynamics. 2023;31(4)

Article DOI: 10.18500/0869-6632-003050

About theory of hybride TWTO and an amplifire with a complex permittivity

A. A. Funtov

Saratov State University, Russia
E-mail: ✉aafuntov@mail.ru

Received 6.03.2023, accepted 5.04.2023, available online 18.07.2023, published 31.07.2023

Abstract. The *purpose* of this work is to construct a nonlinear theory of a hybrid between travelling wave tube (TWT) and an amplifier with a complex permittivity. *Methods.* The following model is considered: an ion-compensated one-dimensional electron beam penetrates the input travelling wave tube section, then flies into a medium with a complex permittivity, and then enters the output travelling wave tube section. A linear theory of this hybrid is constructed, and its results are compared with the results of the well-known linear theory of travelling wave tube. A nonlinear theory of this hybrid was constructed by a modified wave method, and the results were compared with the nonlinear travelling wave tube theory obtained by the classical Ovcharov–Solntsev's wave method. In addition, to test the limits of applicability of the obtained results, a stationary nonlinear theory of the hybrid was constructed, obtained using the large particle method. The results of this theory were also compared with the stationary nonlinear travelling wave tube theory constructed using the large particle method. *Results and conclusion.* Based on the results of the developed theories, it is shown that, under certain parameters, the linear theory and nonlinear theories (both by the modified Ovcharov–Solntsev's wave method and by the large particle method) make it possible to obtain comparable results both in the case of a classical travelling wave tube and for the hybrid under study. It is shown that under certain parameters, due to the resistive instability, the bunching of electrons can be noticeably improved and, as a result, the gain of the hybrid can exceed the gain in a classical travelling wave tube with the same parameters and the same total length of the device in the linear mode of operation. In the nonlinear mode of operation, the specified hybrid, with optimal environmental parameters, can have significantly higher values of output power and efficiency than travelling wave tube with the same value of the space charge parameter and the Pierce parameter.

Keywords: resistive wall amplifier, metamaterial, travelling wave tube.

Acknowledgements. The author is grateful to associate professor V. N. Titov for valuable advice and discussion of the results.

For citation: Funtov AA. About theory of hybride TWTO and an amplifire with a complex permittivity. Izvestiya VUZ. Applied Nonlinear Dynamics. 2023;31(4):452–468. DOI: 10.18500/0869-6632-003050

Introduction

The issues of improving output parameters through the use of metamaterials are important for vacuum microwave electronics and accelerators [1]. Also, the works devoted to various variants and modifications of slow-wave structure (SWS) in TWT (including those with metamaterials) are still relevant and in demand.

For example, as shown in the work [2], it is possible to load the RS TWT with a metamaterial with a negative permittivity. The numerical experiment was carried out at a frequency of 48 GHz at a constant current of 200 mA and a beam radius equal to half the radius of the region in which the electron stream is moving. It is shown that with the studied parameters, a gain factor of 29 dB is possible in a loaded TWT, which significantly exceeds the gain in an unloaded TWT.

On the other hand, it is possible to make a metamaterial out of RS. In [3], an TWT amplifier operating at a frequency of 92 GHz is modeled on the basis of a planar slow-wave structure , which is a metamaterial of meanders. The model used a cylindrical electron flow with an accelerating potential of 16 kV and a current of 60 mA, a magnetic field with an induction of 0.35 T was used. Numerical experiment showed that the maximum gain factor for the parameters under consideration is 36.4 dB, and in the 5 GHz bandwidth — 30 dB. An output power of 17.4 kW is recorded at a frequency of 92 GHz.

In this paper, a hybrid TWT with an amplifier with a complex permittivity (hereinafter CP) is proposed[1]. As is known from the classical theory of the resistive-wall amplifier [4–6], it needs a modulating and removable device. In the first experiments, both resonators and spiral segments [5] were used for this purpose. The point of the CP insertion is to improve the grouping due to the interaction of the beam with the fields of the induced charge in the medium.

As far as is known, there have been no attempts to build this hybrid. Previously (including by the author of this work), a resistive-wall amplifier with a modulating and removable device in the form of spiral segments was considered in the approximation of a given field on the modulator and a given current on the puller (the results have not been published). It is shown that if the medium has active or inductive conductivity, then the gain factor is significantly higher than for a vacuum drift tube. In addition, it is unknown about attempts to create a nonlinear theory of a resistive-wall amplifier with spiral segments as modulating and removable devices.

The purpose of this work is to build a theory of a hybrid of TWT and CP amplifier (TWT – medium with CP – TWT)[2], as well as an approximate nonlinear theory based on the modified Ovcharov-Solntsev wave method.

1. Classical linear theory

First of all, let's build a classical linear theory of a hybrid TWT and a resistive-wall amplifier. We use the following model: an ion-compensated one-dimensional electron stream penetrates the input TWT section, then flies into the medium with the CP, and then enters the output TWT section. We assume that the first TWT plays the role of a modulator and can work in the Kompfner dip. The second TWT is working normally. We assume that the characteristics of the TWT sections, unless otherwise specified, are the same.

Note that for the CP section, in which there is no RS, and therefore no RF field in it, enter

[1]Note that an amplifier with a complex permittivity is one of the variants of a well-known resistive-wall amplifier.

[2]The electron stream penetrates the input TWT section, then flies into the medium with the CP, and then enters the output TWT section.

the coordinate and the space charge (SC) in the usual way for TWT[3] it does not seem convenient, so the following normalization is used: $F(\xi) = E(x)\, e^{j\beta_e x}/(2\beta_e V_0)$ — the dimensionless amplitude of the field in RS (E— dimensional electric field strength), $C = \sqrt[3]{I_0 K/(4V_0)}$— Pierce gain parameter, I_0 — average beam current, K — SWS coupling resistance, V_0 — accelerating voltage, $\beta_e = \omega/v_0$, ω — operating frequency, v_0 — average beam velocity, $N = \beta_e x/(2\pi)$, $\xi = 2\pi CN/C = \beta_e x$, $\omega_p^2 = e\rho_0/(m\varepsilon_0)$ — the square of the plasma frequency, ρ_0 — average charge density in the beam, $j = \sqrt{-1}$, $b = (v_0 - v_f)/v_{ph}$ — desynchronism parameter, v_{ph} — phase wave velocity in a beam-free space, ε_0 — permittivity of vacuum, e/m— specific electron charge, $q = (\omega_p/\omega)^2$ — the SC parameter.

Since the RS is not present in the TWT section, we will use the method of the dispersion equation to calculate the current disturbance. The initial conditions for the second and third sections are the current and its derivative at the end of the previous one. We assume that an unmodulated beam flies into the first TWT and an input signal is applied to it. In the second TWT, in addition to the current condition, equality to zero of the initial disturbance of the electric field strength is added.

With a small gain parameter $C \ll 1$ and in the absence of distributed losses in the RS in the first TWT section (in the normalization of this work), the field in the SWS is determined by the following expression [7]:

$$F = F_0 \left[\frac{\left(\delta_1^2 + q\right) e^{\xi\delta_1}}{(\delta_1 - \delta_2)(\delta_1 - \delta_3)} + \frac{\left(\delta_2^2 + q\right) e^{\xi\delta_2}}{(\delta_2 - \delta_3)(\delta_2 - \delta_1)} + \frac{\left(\delta_3^2 + q\right) e^{\xi\delta_3}}{(\delta_3 - \delta_1)(\delta_3 - \delta_2)} \right], \tag{1}$$

where F_0 is the input signal, δ_i is the roots of the normalized dispersion equation

$$(\delta + jb)\left(\delta^2 + q\right) = -j(1+b)^2 C^3, \tag{2}$$

since the roots of the non-normalized dispersion equation have the form $\beta_e(1 + j\delta)$. Note that this type of δ_i, q and b allows not only to exclude the influence of the Pierce parameter C on the parameters of out-of-sync and SC, but also simplifies subsequent calculations, keeping the form of expressions close to the usual record. In order to get the usual values of the parameters of SC and out of sync, q and b in this normalization must be divided into C^2 and C, respectively. The variable normalized by $I_0 e^{-j\beta_e x}$ current at the beginning of the CP section is found from

$$I(0) = jF_0 \left[\frac{e^{l_1\delta_1}}{(\delta_1 - \delta_2)(\delta_1 - \delta_3)} + \frac{e^{l_1\delta_2}}{(\delta_2 - \delta_3)(\delta_2 - \delta_1)} + \frac{e^{l_1\delta_3}}{(\delta_3 - \delta_1)(\delta_3 - \delta_2)} \right], \tag{3}$$

where l_1 is the normalized length of the 1st TWT.

From the linear theory of the resistive-wall amplifier [6], the expression is valid for alternating current in the CP section

$$I(\xi) = \frac{1}{j(\psi_1 - \psi_2)} \left[-\left(I'(l_1) + j\psi_2 I(l_1)\right) e^{-j\psi_1(\xi - l_1)} + \left(I'(l_1) + j\psi_1 I(l_1)\right) e^{-j\psi_2(\xi - l_1)} \right], \tag{4}$$

where $\psi_{1,2} = \pm\sqrt{q/\varepsilon}$ — the normalized roots of the corresponding dispersion equation taking into account the introduced current normalization.

To calculate the CP, we will use the Drude model

$$\varepsilon = 1 - \frac{\omega_{pM}^2}{\omega(\omega + j\gamma)}, \tag{5}$$

[3] That is, with the Pierce parameter.

where ω_{pM}^2 is the square of the plasma frequency of the medium/metamaterial, γ is the attenuation coefficient. If you enter $\Gamma = \left(\frac{\gamma}{\omega}\right)^2$ and $s = \left(\frac{\omega_{pM}}{\omega}\right)^2$, then the CP can be written as

$$\varepsilon = 1 - \frac{s}{1 + j\Gamma}\,. \tag{6}$$

For the second TWT section, the amplitudes of the partial current waves are found using the solution of the system

$$\begin{pmatrix} 1 & 1 & 1 \\ \delta_1 & \delta_2 & \delta_3 \\ \delta_1^2 + q & \delta_2^2 + q & \delta_3^2 + q \end{pmatrix} I = \begin{pmatrix} I(0)_p \\ I'(0)_p \\ 0 \end{pmatrix} \tag{7}$$

by the Kramer method, where $I(0)_p$, $I'(0)_p$ — the current and its derivative at the output of the CP section obtained from the equation (4), and the index «p» denotes the 2nd TWT. The third equation (in fact, this is the equation of the grouped current) corresponds to the absence of an input signal in the 2nd TWT.

The gain factor will be defined as

$$G = 20\lg\left|\frac{F}{F_0}\right| = 20\lg\left|\frac{1}{jF_0}\left(qI(l_2)_p + \frac{d^2I(l_2)_p}{d\xi^2}\right)\right|, \tag{8}$$

where l_2 — the normalized length of the 2nd TWT.

Let's introduce the values h_1 and h_2 — coordinates of the beginning and end of the TWT section in fractions of the total length of the hybrid. For example, if $h_1 = 0.15$, $h_2 = 0.6$, then the input TWT occupies the first 15% of the total length ($l_1 = 0.15\beta_e x$, where x is the length of the hybrid), the CP section is $h_2 - h_1 = 0.45$, that is 45% of the total length, and the output TWT is— the remaining 40% ($l_2 = 0.4\beta_e x$).

As a reference, we take the parameters from the article [9], which provides data from a full-scale experiment for TWT with a frequency of 220 GHz, a current of 52.4 mA, an accelerating potential of 20.5 kV, a coupling resistance of 1.6 ohms (and, accordingly, $C = 0.01$), a length of RS (excluding the length of the absorber) — 53 mm and a span channel radius of 0.12 mm. Taking into account the geometry of the RS (folded waveguide) $CN = 1.44$.

Let's compare three options: 1 — classical TWT without gap and local absorber; 2— specified hybrid (TWT – CP – TWT); 3— TWT with a gap — a vacuum drift gap having the same length and position as the medium with CP in the hybrid TWT – CP – TWT. We assume that they all have the same total length[4]. Such a comparison will clarify and separate the influence of the drift section and the influence of the medium with CP on the processes taking place. By default, we will use the following boundaries of the CP section $h_1 = 0.1$, h_2=0.85.

Note that in Fig. 1 the section boundaries are clearly visible. In addition, you can see how the grouping of electrons changes in them. Recall that in an TWT with a gap in a section without a RS, grouping with a small q is provided only by a ballistic effect, as in the klystron drift space, and therefore the frequency of current changes should be expected.

From Fig. 2 it can be seen that the hybrid (as well as the TWT with a gap) weakly depends on the desynchronism parameter of the 2nd section, and also that there is no gain in using suppression in the 1st section. This is because with the selected length of the 1st section, the suppression is low (at the level of −0.8 dB) and the Kompfner dip in this section is unattainable

[4]We consider the full length to be the distance from the entrance of the 1st section to the exit of the 3rd.

[4]Для классической ЛБВ просто от параметра рассинхронизма / For a classical TWT, simply from the desynchronism parameter.

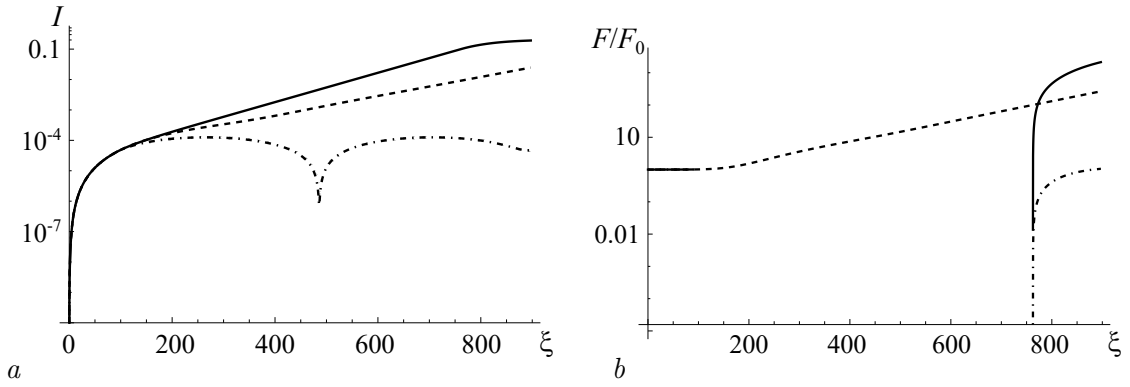

Fig. 1. Dependences (on a logarithmic scale) of the normalized current (a) and the ratio of the field to the input signal (b) on the normalized coordinate. Here and below: solid line — hybrid, dotted line — travelling wave tube (TWT), dash-dotted line — TWT with a break. At $b = b_1 = 0$, $q = 5 \cdot 10^{-5}$, $F_0 = 10^{-8}$, $s = 1.4$, $\Gamma = 5 \cdot 10^{-3}$

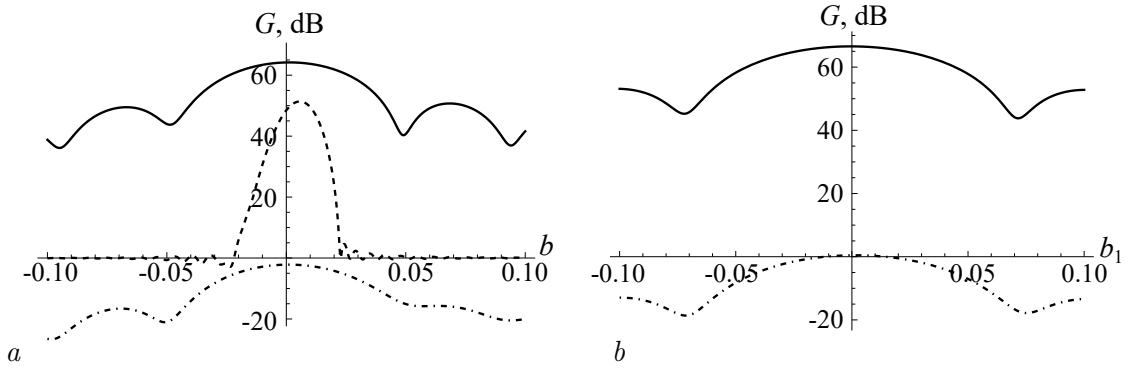

Fig. 2. Dependences of G on the desynchronism parameter of the 2nd section[5] with the 1st section operating in the suppression mode $b_1 = -0.029$ (a), and at $b = 0$ on the desynchronism parameter of the 1st section (b); at $q = 5 \cdot 10^{-5}$, $F_0 = 10^{-8}$, $s = 1.4$, $\Gamma = 5 \cdot 10^{-3}$

with the selected parameters[5]. It is also seen that with the selected parameters, the G of the hybrid is greater than that of the classical TWT in the optimum. Further, we assume that the parameters of the out-of-sync of both TWT sections are the same, that is, $b = b_1$.

It should be noted that in the work [9] $G = 31.2$ dB. However, the TWT with a local absorber is considered there, and neither its length nor position are specified precisely, nor are the values specified that allow calculating the parameter of the q. In addition, the length required for calculations is not specified precisely and the selected value is the result of evaluating the data of the article [9].

As can be seen from Fig. 3–4, there are conditions for the dependence of the optimum on the properties of the CP section. As in the linear theory of TWT, the location and length of the local absorber are important, so the CP section is important for the hybrid under consideration. From Fig. 3 it can be seen that at low q, when convective instability prevails in the TWT sections, it is most important to group the beam by increasing the proportion of the first TWT (lower right corner in Fig. 3, a). With an increase in q, convective instability gives way to the main role of resistive instability, and an optimum appears with a sufficiently long CP section (upper left corner in Fig. 3, b).

[5]The modes of effective modulation of the electron flow in terms of velocity in the first section, when a significant part of the energy of the electromagnetic wave is transmitted to the electron flow, were not considered, since they require a significantly longer length of the modulator section.

Thus, for small q, in order to achieve an optimum, almost half of the length should fall on the modulator, the same amount — on the medium with CP, and the remaining short area — on the output TWT. For large q — a short modulator, a long area of the medium with CP and a short area of the output TWT.

One of the possible implementations of the CP section is the use of a structure of meander segments located at the same distance from each other along the beam (above and below it) and oriented perpendicular to the beam [8] (fig. 3, *c*). In the case of a correctly selected distance between the meanders, as well as their sizes, the beam "sees"the medium with a negative real part of the effective CP. In the case of Fig. 3, *c* the input TWT section should be located on the right and the output section on the left. The problem of correctly connecting sections can be quite a difficult, but technically feasible task, and therefore goes beyond the scope of this work and will not be considered.

From Fig. 4 the influence of the properties of the medium on the gain is visible. The highest value of the gain, as expected, is observed near the resonance $s = 1$ at a sufficiently small Γ. This resonance, as in the theory of a resistive-wall amplifier, can be explained (by analogy with [10]) as follows: bias currents and inductive currents in the medium become equal to each other in magnitude, and the induced charge tends to infinity. In this case, the region of a higher gain factor at $s > 1$ can be explained by the fact that the forces in the beam and the forces created by the induced charge turn out to be in opposite phases, which leads to an improvement in the conditions for grouping electrons in the beam. And the region of a lower gain at $s < 1$ is due to the fact that the intensity of the electric field created by the induced charge is in phase with the forces of the q in the beam. As a result, the longitudinal repulsion of electrons increases and the amplification of the spatial charge wave turns out to be impossible.

In addition, for some Γ and s, a suppression zone appears (see, for example, Fig. 4, *b*). In this zone, the medium is not a metamaterial and has a real part of ε close to one. With the change of CN and q, the coordinates of the suppression and its depth change. From Fig. 4, *c* it can be seen that with the selected parameters in the suppression zone, the hybrid exhibits behavior similar to TWT with gap (similar to the ballistic effect), and the grouping is much worse than in the case of a metamaterial, and is comparable to grouping in a vacuum drift space. Thus, this effect is not explained only by the influence of the attenuation parameter in the Γ environment. In this zone, the grouping in the medium seems to deteriorate due to the longitudinal repulsion of electrons.

From Fig. 5 it can be seen that with a small q, the gain of the classical TWT near $b = 0$ exceeds the gain of the hybrid, and as the q increases vice versa. From this, it can be concluded that two instabilities inherent in TWT and CP operate in the hybrid, and with a small q, convective instability prevails in TWT sections.

The presence of a CP environment, as can be seen from Fig. 5, makes the device less sensitive to the desynchronism parameter (the area of positive G increases with the growth of b). It is also seen that in the area of relatively small out-of-sync, the gain in TWT is greater than that of the hybrid, and the area where the gain is greater than that of the hybrid increases with the growth of q.

2. Modification of the Ovcharov-Solntseva wave method

In this section, we study the same model as in section 1: an ion-compensated one-dimensional electron stream penetrates the input TWT section, then flies into the medium with a CP, and then enters the output TWT section. We assume that all electrons of a given cross-section of the

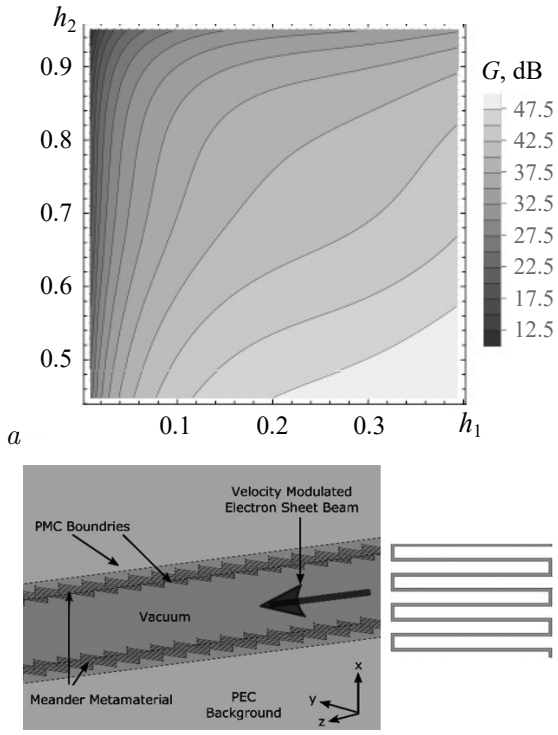

Fig. 3. Dependences of G on the boundaries of the CP[7] section (a, b) and an example of a possible implementation of the CP section from meander segments (from [8]) (c). At $b = b_1 = 0$, $F_0 = 10^{-8}$, $s = 1.4$, $\Gamma = 5 \cdot 10^{-3}$; $q = 10^{-5}$ (a), $q = 5 \cdot 10^{-5}$ (b)

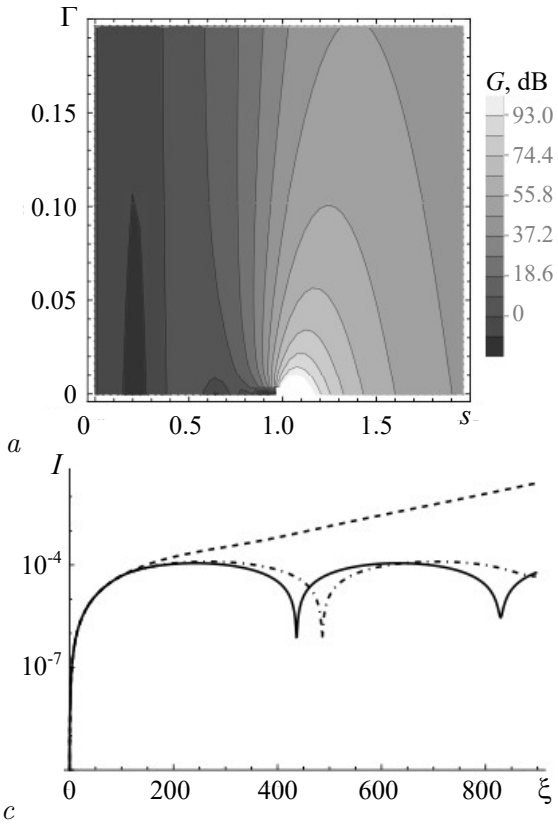

Fig. 4. Dependences of G on the properties of the CP section (a, b) and dependence of the current on the length (c) at b=b_1=0, $q = 5 \cdot 10^{-5}$, $F_0 = 10^{-8}$; $\Gamma = 5 \cdot 10^{-3}$ (b, c); $s = 0.212$ (c)

beam are affected by the same cross-section averaged electric field, and that the movement of electrons is unidirectional. In addition, it is assumed that the modulation of electrons in velocity is small, but there are no restrictions on the depth of modulation of the electron beam in current and density. We assume that the characteristics of the TWT sections (except for the length) are the same.

Following the [11] method of operation, we use the following nonlinear TWT equations in Lagrange variables as initial ones, taking into account the previously introduced normalization:

$$-\frac{\partial^2\theta}{\partial\xi^2} = \mathrm{Re}\left[Fe^{j(\omega t_0+\theta)} + \sum_{n=1}^{\infty}\frac{jp_n^2}{n}qI_ne^{jn(\omega t_0+\theta)}\right], \tag{9}$$

$$\frac{dF}{d\xi} + jbF = -(1+b)^2C^3I_1, \tag{10}$$

$$I_n = \frac{1}{\pi}\int_0^{2\pi} e^{-jn(\omega t_0+\theta)}d(\omega t_0), \tag{11}$$

where $\theta(\xi, t_0)$— perturbation of the electron flight angle under the action of the field, $p_n^2 = n^2/(n^2+k^2)$, $k = 2/(\beta_e r)$— normalized inverse beam radius (r — respectively, the dimensional radius of the beam), t_0— the time of entry of electrons into the interaction space, I_n— normalized amplitude of the n th harmonic of the current.

Let's imagine a perturbation of the electron flight angle under the action of a field in the form of a Fourier series:

$$\theta = \frac{\theta_0(\xi)}{2} + \mathrm{Re}\sum_{m=1}^{\infty}\theta_m e^{jm\omega t_0}, \tag{12}$$

where is $\theta_m(x) = \frac{1}{\pi}\int_0^{2\pi}\theta(x,t_0)\,e^{-jm\omega t_0}d(\omega t_0)$. Multiply (9) by $\frac{1}{\pi}e^{-jm\omega t_0}$ and integrate t_0 from

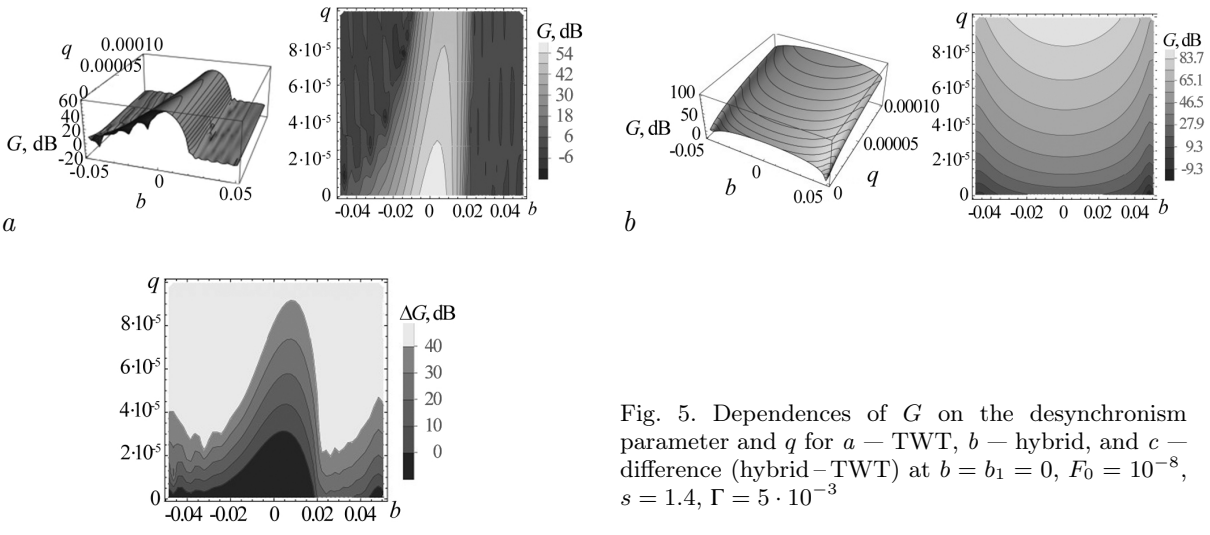

Fig. 5. Dependences of G on the desynchronism parameter and q for a — TWT, b — hybrid, and c — difference (hybrid – TWT) at $b = b_1 = 0$, $F_0 = 10^{-8}$, $s = 1.4$, $\Gamma = 5\cdot 10^{-3}$

0 to 2π, then taking into account (12) we get:

$$-\frac{\partial^2\theta_m}{\partial\xi^2} = \frac{1}{\pi}\int_0^{2\pi} \mathrm{Re}\left[Fe^{j(\omega t_0+\theta)}\right] e^{-jm\omega t_0} d(\omega t_0) + \\ + \frac{1}{\pi}\int_0^{2\pi} \mathrm{Re}\left[\sum_{n=1}^{\infty} \frac{jp_n^2}{n} qI_n e^{jn(\omega t_0+\theta)}\right] e^{-jm\omega t_0} d(\omega t_0). \quad (13)$$

To approximate the calculation of integrals, we limit ourselves to the 1st term in the equation (12) and introduce

$$\theta = \frac{\theta_0}{2} + \mathrm{Re}\left[Be^{j\omega t_0}\right]. \quad (14)$$

Then in the equation (11) we get

$$I_n = \frac{1}{\pi}\int_0^{2\pi} e^{-jn\left(\omega t_0+\frac{\theta_0}{2}+Re\left[Be^{j\omega t_0}\right]\right)} d(\omega t_0). \quad (15)$$

Using the notation introduced earlier for $m = 0$, the equation (13) will take the form

$$-\frac{\partial^2\theta_0}{\partial\xi^2} = \frac{1}{\pi}\int_0^{2\pi} \mathrm{Re}\left[Fe^{j\left(\omega t_0+\frac{\theta_0}{2}+\mathrm{Re}\left[Be^{j\omega t_0}\right]\right)}\right] d(\omega t_0) + \\ + \sum_{n=1}^{\infty} q\frac{p_n^2}{n}\frac{1}{\pi}\int_0^{2\pi} \mathrm{Re}\left[jI_n e^{jn\left(\omega t_0+\frac{\theta_0}{2}+\mathrm{Re}\left[Be^{j\omega t_0}\right]\right)}\right] d(\omega t_0). \quad (16)$$

For $m = 1$, the equation (13) will take the form

$$-\frac{\partial^2 B}{\partial\xi^2} = \frac{1}{\pi}\int_0^{2\pi} \mathrm{Re}\left[Fe^{j\left(\omega t_0+\frac{\theta_0}{2}+\mathrm{Re}\left[Be^{j\omega t_0}\right]\right)}\right] e^{-j\omega t_0} d(\omega t_0) + \\ + \sum_{n=1}^{\infty} q\frac{p_n^2}{n}\frac{1}{\pi}\int_0^{2\pi} \mathrm{Re}\left[jI_n e^{jn\left(\omega t_0+\frac{\theta_0}{2}+\mathrm{Re}\left[Be^{j\omega t_0}\right]\right)}\right] e^{-j\omega t_0} d(\omega t_0). \quad (17)$$

For the CP section, in which there is no RS, and therefore no RF field in it, the number of basic equations decreases: the equation remains (15), and the expressions for the components of the electron flight angle take the form

$$-\frac{\partial^2\theta_0}{\partial\xi^2} = \sum_{n=1}^{\infty} q\frac{p_n^2}{n}\frac{1}{\pi}\int_0^{2\pi} \mathrm{Re}\left[\frac{j}{\varepsilon}I_n e^{jn\left(\omega t_0+\frac{\theta_0}{2}+\mathrm{Re}\left[Be^{j\omega t_0}\right]\right)}\right] d(\omega t_0), \quad (18)$$

$$-\frac{\partial^2 B}{\partial\xi^2} = \sum_{n=1}^{\infty} q\frac{p_n^2}{n}\frac{1}{\pi}\int_0^{2\pi} \mathrm{Re}\left[\frac{j}{\varepsilon}I_n e^{jn\left(\omega t_0+\frac{\theta_0}{2}+\mathrm{Re}\left[Be^{j\omega t_0}\right]\right)}\right] e^{-j\omega t_0} d(\omega t_0). \quad (19)$$

Taking into account the time harmonic decomposition, the CP will take the form

$$\varepsilon(n) = 1 - \frac{s_M}{n\,(n + j\Gamma)}. \tag{20}$$

If we decompose B into a module and a phase, then the equation (15) will take the form

$$I_n = 2J_n\,(n\,|B|)\,e^{-jn\left(\frac{\theta_0}{2}+\frac{\pi}{2}-ArgB\right)}. \tag{21}$$

And the equations (16), (17) and (10) will be written as

$$\frac{dF}{d\xi} + jbF = -(1+b)^2 C^3 2J_1\,(|B|)\,e^{j\left(ArgB-\frac{\theta_0}{2}-\frac{\pi}{2}\right)}, \tag{22}$$

$$\frac{\partial^2\theta_0}{\partial\xi^2} = -J_1\,(|B|)\,2\,\mathrm{Re}\left(Fe^{-j\left(ArgB-\frac{\pi}{2}-\frac{\theta_0}{2}\right)}\right), \tag{23}$$

$$\begin{aligned}\frac{\partial^2 B}{\partial\xi^2} = -\Big[&FJ_0\,(|B|)\,e^{j\frac{\theta_0}{2}} + F^*J_2\,(|B|)\,e^{-j\left(\frac{\theta_0}{2}-2\left[ArgB-\frac{\pi}{2}\right]\right)} + \\ &+ 2j\sum_{n=1}^{\infty} qJ_n\,(n\,|B|)\,e^{jn\left(ArgB-\frac{\pi}{2}\right)}\frac{p_n^2}{n}\,(J_{n-1}\,(n\,|B|) - J_{n+1}\,(n\,|B|))\Big],\end{aligned} \tag{24}$$

where the "*"sign indicates a complex conjugation. The equations (18) and (19) are written as

$$\frac{\partial^2\theta_0}{\partial\xi^2} = -2j\sum_{n=1}^{\infty} q\frac{p_n^2}{n}J_n^2\,(n\,|B|)\left(\frac{1}{\varepsilon} - \frac{1}{\varepsilon^*}\right), \tag{25}$$

$$\frac{\partial^2 B}{\partial\xi^2} = -2j\sum_{n=1}^{\infty} q\frac{p_n^2}{n}J_n\,(n\,|B|)\,e^{jn\left(ArgB-\frac{\pi}{2}\right)}\left(\frac{J_{n-1}\,(n\,|B|)}{\varepsilon(n)} - \frac{J_{n+1}\,(n\,|B|)}{\varepsilon^*(n)}\right). \tag{26}$$

Thus, the TWT section is described by a system of equations (22)–(24), and the CP section is described by the equations (25) and (26).

As the initial conditions for the first (input) TWT section, we take

$$F\,(0) = F_0, \quad B\,(0) = 0, \quad \frac{dB\,(0)}{d\xi} = 0, \quad \theta_0\,(0) = 0. \tag{27}$$

For the CP section, the initial conditions will be

$$\frac{dB\,(0)}{d\xi} = \left.\frac{dB}{d\xi}\right|_{TWT_1}, \quad B\,(0) = B|_{TWT_1}, \quad \frac{d\theta_0\,(0)}{d\xi} = \left.\frac{d\theta_0}{d\xi}\right|_{TWT_1}, \quad \theta_0\,(0) = \theta_0|_{TWT_1}. \tag{28}$$

The initial conditions in the second (output) TWT section will take the form

$$\frac{dB\,(0)}{d\xi} = \left.\frac{dB}{d\xi}\right|_{CP_1}, \quad B\,(0) = B|_{CP_1}, \quad \frac{d\theta_0\,(0)}{d\xi} = \left.\frac{d\theta_0}{d\xi}\right|_{CP_1}, \quad \theta_0\,(0) = \theta_0|_{CP_1}, \quad F\,(0) = 0. \tag{29}$$

We will search for the gain factor using the formula

$$G = 20\lg\left|\frac{F}{F_0}\right|. \tag{30}$$

With the selected parameters, the results obtained by the wave method with a weak signal show a good agreement with the results of linear theory in a fairly large range of parameters

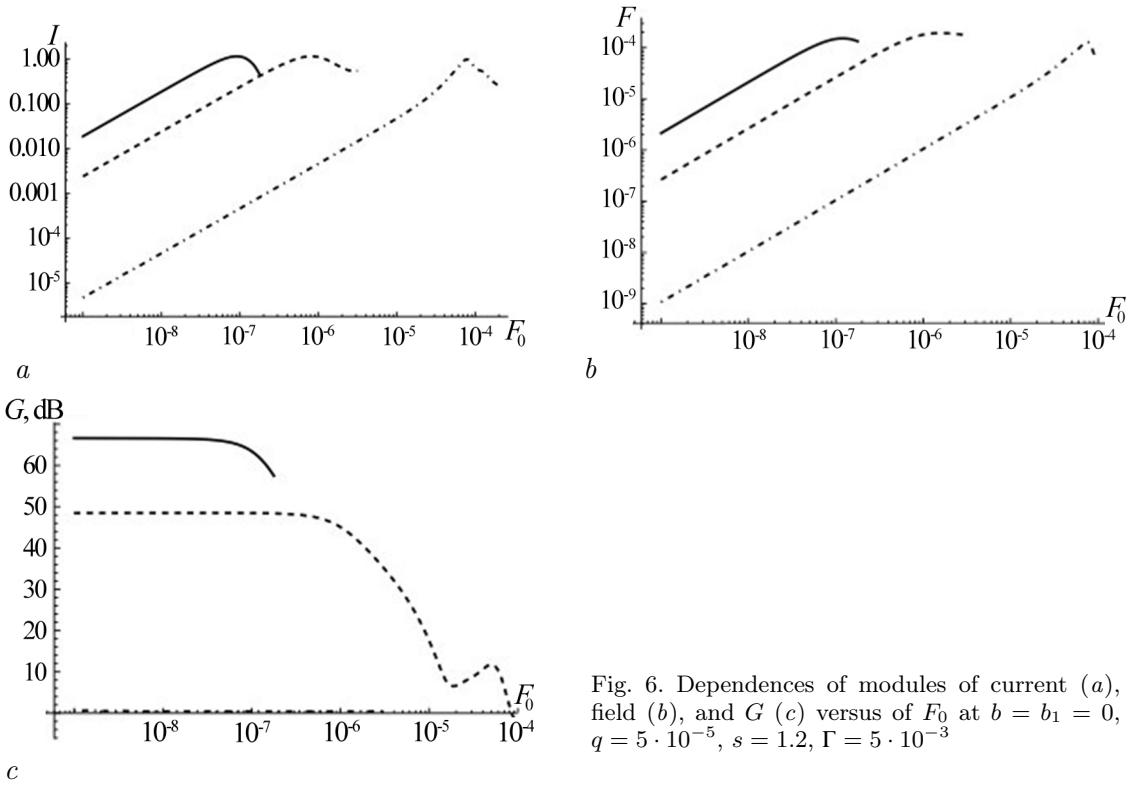

Fig. 6. Dependences of modules of current (a), field (b), and G (c) versus of F_0 at $b = b_1 = 0$, $q = 5 \cdot 10^{-5}$, $s = 1.2$, $\Gamma = 5 \cdot 10^{-3}$

with the following features. Depending on the gain from the boundaries of the CP section, unlike Fig. 3 in nonlinear theory, the optima appear more clearly and are shifted to the appropriate angles. Also, the dependences of the gain coefficient on the desynchronism parameter coincide well in both theories at $|b| < 0.03$[8]. At $|b| > 0.03$, apparently The features of the wave method are revealed, or rather, the limits of its applicability due to the discarded terms. Perhaps there is a imbalance between the braking of the entire beam and the movement of particles in the beam.

From Fig. 6 it can be seen that the hybrid has the best grouping — the value of the parameter B corresponding to the maximum current is achieved at a lower input power, and the gain of the hybrid is significantly higher than that of the TWT. For TWT with discontinuity, due to the short length of the modulator, the electrons did not have time to sufficiently change their velocity relative to the wave and therefore the gain is negligible compared to other cases, and in the future we will not consider TWT with discontinuity. The graphs also show the limit of applicability of the method, that is, when all harmonics except the first one can be discarded, namely until the current exceeds 1.16 — the value due to the properties of the Bessel function, and therefore the dependencies behind this value are not considered.

3. Stationary nonlinear theory (large particle method)

Let's consider the results of the stationary nonlinear theory for the TWT-CP-TWT hybrid obtained by the large particle method and compare them with those given earlier. In the TWT section, we use the approximation of the reduction coefficient [12] and the basic equations from

[8]Note that this value of the desynchronism parameter in the usual TWT normalization is 2.98.

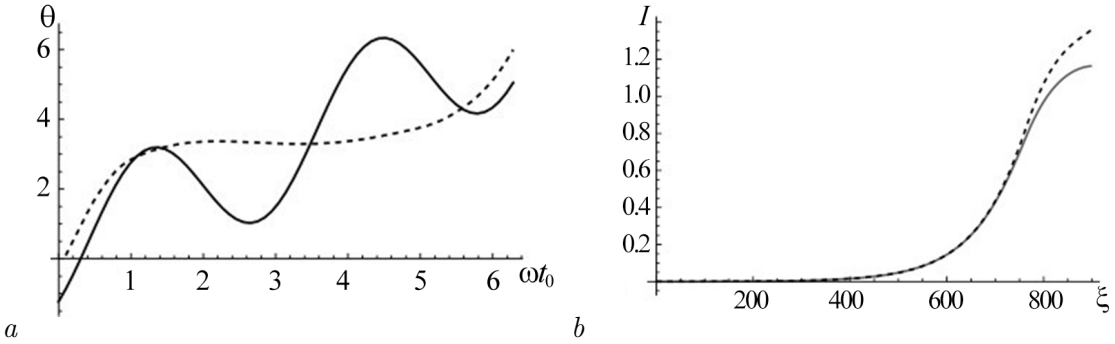

Fig. 7. Dependence of the transit angle perturbation on the initial phase in the hybrid (a) and distribution of the 1st harmonic of the current over the full length of the hybrid (b) at $F_0 = 8.9 \cdot 10^{-8}$, $s = 1.4$, $\Gamma = 5 \cdot 10^{-3}$, $q = 5 \cdot 10^{-5}$, $b = 0$. Solid line is based on the wave method, the dotted line is based on the large particle method

[13], which will take the form for the nth particle:

$$\frac{\partial^2 \theta_n}{\partial \zeta^2} = -(2\pi N)^2 \left(1 + \frac{1}{2\pi N}\frac{\partial \theta_n}{\partial \zeta}\right)^3 \mathrm{Re}\left[F e^{j\theta_n} + jq \sum_{m=1}^{M} \frac{R_m e^{jm\theta_n}}{m} \left(\sum_{n}^{N_p} \frac{2e^{-jm\theta_n}}{N_p}\right)\right], \quad (31)$$

$$\frac{\partial F}{\partial \zeta} + 2j\pi N b F = -2C^3 N \sum_{n}^{N_p} \frac{2\pi}{N_p} e^{-jm\theta_n}, \quad (32)$$

where $\zeta = x/l$, l is the length of the interaction space in meters, N_p — the number of large particles, M — the number of harmonics studied, R_n — reduction factor. For all the presented results, $N_p = 64$, $M = 7$.

For the CP section, the equation of motion of the nth particle will take the form

$$\frac{\partial^2 \theta_n}{\partial \zeta^2} = -(2\pi N)^2 \left(1 + \frac{1}{2\pi N}\frac{\partial \theta_n}{\partial \zeta}\right)^3 \mathrm{Re}\left[jq \sum_{m=1}^{M} \frac{R_m e^{jm\theta_n}}{m\varepsilon(m)} \left(\sum_{n}^{N_p} \frac{2e^{-jm\theta_n}}{N_p}\right)\right]. \quad (33)$$

As boundary conditions, we assume that θ and $\partial\theta/\partial\zeta$ are continuous at the ends of the sections, and there is no RF field at the entrance to the second TWT section.

In the present work, an infinitely wide beam was mainly studied. To take into account the finiteness of filling, it is necessary to calculate R_n using the formula [13]

$$R_n = \left(1 + \frac{7.5214(r/a)^2 - 4.3178\,(r/a) + 2.4895}{n^2 \beta_e^2 r^2}\right)^{-1}, \quad (34)$$

where a is the radius of the span channel.

With a weak signal, the results of the large particle method match well with those presented above, and therefore are not given. Of greater interest is hybrid analysis for relatively large signals.

It should be noted that the grouping of electrons (including in a hybrid) predicted by the wave method and the large particle method differs significantly. While the grouping is relatively small, the first harmonic currents predicted by these methods coincide, however, with an increase in the input signal, as can be seen from Fig. 7, noticeable differences begin: the number and "place"of clots formation differ. In addition, closer to the output, the first harmonic current

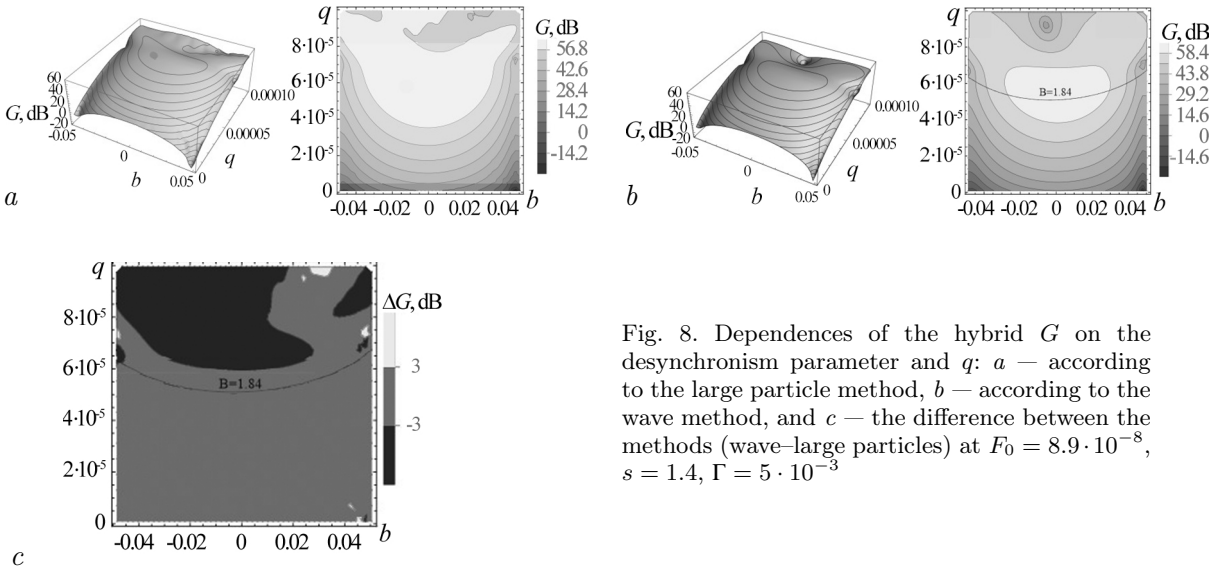

Fig. 8. Dependences of the hybrid G on the desynchronism parameter and q: a — according to the large particle method, b — according to the wave method, and c — the difference between the methods (wave–large particles) at $F_0 = 8.9 \cdot 10^{-8}$, $s = 1.4$, $\Gamma = 5 \cdot 10^{-3}$

predicted by the large particle method exceeds the calculations using the wave method. Thus, despite the fact that the wave method and the large particle method describe a significantly different grouping in the model under study, "integrally"(that is, in terms of the first harmonic current and, consequently, the gain) they (as will be shown below) show a good match in a fairly wide range of parameters.

In Fig. 8 the results of both methods under consideration and their difference are shown. It can be seen that with relatively large input signals in the range under consideration, there is a clear optimum, the position and values of G in which both methods describe quite consistently. Therefore, it can be assumed that it is mainly the 1st harmonic that contributes to it. Also, with increasing frequency response, both methods predict an area of noticeable deterioration of the grouping (which occurs when $B > 1.84$ in the wave method, that is, beyond the first maximum of the 1st harmonic of the current), but indicate its different location. It can be assumed that higher harmonics are beginning to significantly influence there and the wave method has gone beyond assumptions. Thus, the wave method allows us to estimate the boundaries of an area where taking into account only the 1st harmonic is not enough.

We present estimates of the output parameters of the hybrid and TWT in the case of an infinitely wide beam and with a finite full filling of the span channel. The output power and electronic efficiency are calculated taking into account the introduced normalization using the formulas [14]

$$P_{\text{out}} = I_0 V_0 \frac{|F|^2}{2^3} \quad \text{и} \quad \eta = \frac{|F|^2}{2^3}. \tag{35}$$

As can be seen from the table. 1, with the selected (relatively rough) methods of accounting for the finiteness of the beam filling, considered in the case of full filling, the hybrid shows comparable output characteristics (G, power and efficiency) with the classical TWT, and near, and not in resonance of the operating frequency with the frequency of the metamaterial. A slight (versus the wave method) decrease in the gain coefficient using the large particle method can also be explained by the contribution of higher harmonics.

Of course, taking into account incomplete filling, which is more often used in modern microwave devices, will also make its contribution, however, the parameters of real TWT change due to the local absorber, which was not taken into account in the above calculations. Also, it should not be forgotten that for all other frequencies that do not coincide with a narrow band of

Table 1. Gain factor (in linear mode) for hybrid and TWT. The designations correspond to: ∞ — infinitely wide beam, 1 — full filling of the span channel at $F_0 = 10^{-8}$, $q = 5 \cdot 10^{-5}$, $\Gamma = 5 \cdot 10^{-3}$, $s = 1.4$, $b = 0$

	G, дБ	
	∞	1
Modification of the wave method		
TWT	48.5	53.6
Hybrid	66.5	48.8
Modification of the wave method		
TWT	48.5	48.7
Hybrid	66.5	66.4

resonant properties of the medium, the metamaterial will act as a gap with a vacuum drift space usual for TWT.Recall that according to [4–6], one of the advantages of a resistive-wall amplifier is the almost complete absence of feedback between output and input..

In the work [9], the parameters from which were used for calculations, in linear mode, the TWT at a frequency of 220 GHz has a gain factor of 31.2 dB, and with an input signal of 25 MW, the output power is 15 W, with a maximum power of 30 W achieved at a frequency of 217 GHz, and the maximum achievable efficiency is 2.79%. Previously, the local absorber in TWT was not taken into account in the calculations. The evaluation of the data from the article [9] shows that the total length of the lamp, taking into account the absorber in CN, will increase to 1.58, and the absorber itself in the normalization of this work has coordinates $h_1 = 0.328$, $h_2 = 0.42$. In the table. 2 calculations are given with parameters that, without taking into account ohmic losses, allow for TWT to obtain an output power similar to that described in [9]. The local absorber is taken into account as a gap (that is, similar to the hybrid in the case of $s = 0$).

Table 2. The output power and the electronic efficiency for TWT and hybrid, calculated by the method of large particles, in the case of full filling of the span channel at $F_0 = 3.53 \cdot 10^{-5}$ (25 mW), $b = 2.4 \cdot 10^{-2}$, $q = 5.9 \cdot 10^{-5}$, $\Gamma = 5 \cdot 10^{-3}$. The first line contains data from [9]

	P_{out}, Вт	η,%
TWT from [9]	15	1.4[9]
TWT	14.98	1.33
Hybrid $s = 1.35$	17.02	1.52
Hybrid with optimal parameters[10]	75.22	6.94

From the table. 2 it can be concluded that, firstly, replacing the vacuum drift/gap with a medium with a CP while maintaining length and position does not lead to a significant deterioration in output characteristics, but with a properly selected medium they can be improved. Secondly, by selecting the properties of the medium, as well as changing the position and length of the CP section, it is possible to achieve a significant increase in output power and efficiency. In addition, the proposed hybrid can be used in a wider area of synchronization.It is appropriate to recall that in the full-scale experiment [4] the resistive-wall amplifier showed a weak dependence on the accelerating potential of the beam. Output characteristics comparable to TWT in a hybrid can be obtained with a significantly lower input signal, which can be useful, since the power of

[9] Данные для КПД на рассматриваемой частоте 220 ГГц не приводятся, поэтому значение 1.4% является экстраполяцией.

[10] $b = 0.02$, $s = 0.4$, $h_1 = 0.274$, $h_2 = 0.545$, длина, входной сигнал и ПЗ не менялись.

generators (primarily semiconductor ones) is comparatively low at hundreds of gigahertz.

Conclusion

Based on the results of this work, the following conclusions can be drawn.

1. Under certain parameters, the nonlinear theory obtained by the modified Ovcharov-Solntsev wave method allows us to obtain results comparable both to the results of the nonlinear stationary theory obtained by the large particle method and to the results of the linear theory both in the case of classical TWT and for the hybrid under study. This fact indicates its reliability, and also allows us to estimate the area of dominance of the first harmonic.
2. In nonlinear theory, the modified Ovcharov-Solntsev wave method makes an assumption about the nature of the grouping. This explains the differences in the results for some parameters with the nonlinear stationary theory using the large particle method. In other cases, there is a good match.
3. Due to resistive instability, the grouping of electrons can be noticeably improved. And, as a result, the gain of the hybrid can exceed the gain of the classical TWT (both with and without a gap).
4. In the case of a large signal with the parameters under consideration, it is shown that by selecting the properties of the CP section, it is possible to achieve a significant increase in output power and efficiency compared to TWT, and, as a result, it is possible to achieve power and efficiency values comparable to TWT with a smaller input signal.

References

1. Duan Z, Shapiro MA, Schamiloglu E, Behdad N, Gong Y, Booske JH, Basu BN, Temkin RJ. Metamaterial-inspired vacuum electron devices and accelerators. IEEE Transactions on Electron Devices. 2019;66(1):207–218. DOI: 10.1109/TED.2018.2878242.
2. Rashidi A, Behdad N. Metamaterial-enhanced traveling wave tubes. In: IEEE International Vacuum Electronics Conference (IVEC). 22-24 April 2014, Monterey, CA, USA. New York: IEEE; 2014. P. 199–200. DOI: 10.1109/IVEC.2014.6857559.
3. Ulisse G, Krozer V. W-band traveling wave tube amplifier based on planar slow wave structure. IEEE Electron Device Letters. 2017;38(1):126–129. DOI: 10.1109/LED.2016.2627602.
4. Birdsall CK, Brewer GR, Haeff AV. The resistive-wall amplifier. Proceedings of the IRE. 1953;41(7):865–875. DOI: 10.1109/JRPROC.1953.274425.
5. Birdsall CK, Whinnery JR. Waves in an electron stream with general admittance walls. J. Appl. Phys. 1953;24(3):314–323. DOI: 10.1063/1.1721272.
6. Lopukhin VM, Vedenov AA. Absorption amplifier. Sov. Phys. Usp. 1954;53(1):69–86 (in Russian). DOI: 10.3367/UFNr.0053.195405c.0069.
7. Tseitlin MB, Kats AM. Travelling Wave Tube. Moscow: Sovetskoe Radio; 1964. 308 p. (in Russian).
8. Rowe T, Behdad N, Booske JH. Metamaterial-enhanced resistive wall amplifier design using periodically spaced inductive meandered lines. IEEE Transactions on Plasma Science. 2016;44(10):2476–2484. DOI: 10.1109/TPS.2016.2599144.
9. Jiang Y, Lei W, Hu P, Song R, Ma G, Chen H, Jin X. Demonstration of a 220-GHz continuous wave traveling wave tube. IEEE Transactions on Electron Devices. 2021;68(6): 3051–3055. DOI: 10.1109/TED.2021.3075922.
10. Kasatkin LV. On amplification of space charge waves during the passage of electron beams in media with inductive conductivity. Radio Engineering and Electronic Physics. 1961;6(2):

267–274 (in Russian).
11. Ovcharov VT, Solntsev VA. Simplified nonlinear equations of a traveling wave lamp. Radio Engineering and Electronic Physics. 1962;7(11):1931–1940 (in Russian).
12. Datta SK, Kumar L. Plasma frequency reduction factor. Defence Science Journal. 2008;58(6): 768–770. DOI: 10.14429/dsj.58.1705.
13. Branch GM, Mihran TG. Plasma frequency reduction factors in electron beams. IRE Transactions on Electron Devices. 1955;2(2):3–11. DOI: 10.1109/T-ED.1955.14065.
14. Vainshtein LA, Solntsev VA. Lectures on Microwave Electronics. Moscow: Sovetskoe Radio; 1973. 399 p. (in Russian).